

Supporting Information: Fast lithium-ion conductivity in the
'empty-perovskite' $n = 2$ Ruddlesden-Popper-type oxysulfide
 $\text{Y}_2\text{Ti}_2\text{S}_2\text{O}_5$

Kit McColl¹ and Furio Corà¹

¹Department of Chemistry, University College London, 20 Gordon Street, London,
WC1H 0AJ, United Kingdom

January 4, 2021

Contents

1	Supplementary methods	2
1.1	Basis sets	2
1.2	Constrained geometry optimisations for the calculation of activation barriers.	2
2	Supplementary results	3
2.1	Calculated lattice parameters $\text{Y}_2\text{Ti}_2\text{S}_2\text{O}_5$	3
2.2	Bond lengths and interatomic distances in $\text{Y}_2\text{Ti}_2\text{S}_2\text{O}_5$	4
2.3	Changing geometry of TiO_5S octahedra in $\text{Y}_2\text{Ti}_2\text{S}_2\text{O}_5$ at different levels of lithiation .	5
2.4	Electronic density of states for $\text{Y}_2\text{Ti}_2\text{S}_2\text{O}_5$ and $\text{Li}_2\text{Y}_2\text{Ti}_2\text{S}_2\text{O}_5$ calculated using PBEsol.	6

1 Supplementary methods

1.1 Basis sets

All-electron basis sets were used to describe the following atoms: Ti (Ti_86-411(d31)G_darco), S (S_86-3111G**_bredow_2004), O (O_8-411d1_cora_2005), Li (Li_5-11(1d)G_baranek_2013_LiNbO3), Na (Na_8-511(1d)G_baranek_2013_NaNbO3) and Mg (Mg_8-511d1G_valenzano_2006). An effective core pseudopotential was used for the Y atom (Y_POB_DZVP_2018). Basis sets are available from the online repository: (<https://www.crystal.unito.it/basis-sets.php>)

1.2 Constrained geometry optimisations for the calculation of activation barriers.

Activation barriers were determined by running constrained geometry optimisations, using the following procedure. First, the initial and final geometries of the mobile ion in question were determined by full geometry optimisations (lattice parameters and atomic positions). From the initial and final geometry, a series of images along the pathway were created by a linear interpolation of lattice parameter and atomic coordinates. A constrained geometry optimisation was then performed on each image along the pathway. In the constrained optimisation, the movement of the mobile ion in question was constrained along the reaction coordinate. To prevent the entire structure moving with the mobile ion, a single framework ion was also constrained along the direction of motion of the mobile ion; in each case, an S-ion close to the migration pathway was chosen.

2 Supplementary results

2.1 Calculated lattice parameters $\text{Y}_2\text{Ti}_2\text{S}_2\text{O}_5$.

Table S1: Crystal structure parameters and bandgaps of $\text{Y}_2\text{Ti}_2\text{S}_2\text{O}_5$ from experiment, and calculated with different exchange-correlation functionals. The numbers in brackets represent the difference with respect to the experimental results reported by Hyett et al.¹

Method	a (Å)	c (Å)	Vol (Å ²)	ρ (g cm ⁻¹)	Bandgap (eV)
Expt. ¹	3.7696	22.8056	324.06	4.34	1.90
B3LYP	3.7915 (0.6)	23.3140 (2.2)	335.15 (3.4)	4.16	2.45
B3LYP-D3	3.7494 (-0.5)	22.8853 (0.3)	321.72 (-0.7)	4.33	2.44
PBE0	3.7644 (-0.1)	22.8873 (0.4)	324.33 (0.1)	4.30	2.85
PBE0-D3	3.7384 (-0.8)	22.6516 (-0.7)	316.58 (-2.3)	4.40	2.86
PBE	3.7964 (0.7)	23.0168 (0.9)	331.73 (2.4)	4.20	1.08
PBE-D3	3.7689 (0.0)	22.8502 (0.2)	324.58 (0.2)	4.29	1.08
HSE06	3.7634 (-0.2)	22.9247 (0.5)	324.68 (0.2)	4.29	2.19
HSE06-D3	3.7338 (-0.9)	22.6917 (-0.5)	316.34 (-2.4)	4.40	2.19
PBEsol	3.7593 (-0.3)	22.7233 (-0.4)	321.13 (-0.9)	4.39	0.97

2.2 Bond lengths and interatomic distances in $\text{Y}_2\text{Ti}_2\text{S}_2\text{O}_5$.

Table S2: Bond lengths and interatomic distances in $\text{Y}_2\text{Ti}_2\text{S}_2\text{O}_5$ calculated using different functionals. The numbers in brackets give the different with respect to the experimental value, presented in the top data row.

Method	Y-O (Å)	Y-S (Å)	Y-S' (Å)	Ti-O1 (eq) (Å)	Ti-O2 (ax) (Å)	Ti-S (Å)
Expt. ¹	2.433	2.802	2.933	1.943	1.794	2.872
B3LYP	2.467 (1.4 %)	2.825 (0.8 %)	3.005 (2.5 %)	1.959 (0.9 %)	1.807 (0.7 %)	2.963 (3.2 %)
B3LYP-D3	2.439 (0.3 %)	2.791 (-0.4 %)	2.873 (-2.0 %)	1.939 (-0.2 %)	1.795 (0.0 %)	2.926 (1.9 %)
PBE0	2.436 (0.1 %)	2.801 (0.0 %)	2.920 (-0.5 %)	1.943 (0.0 %)	1.796 (0.1 %)	2.901 (1.0 %)
PBE0-D3	2.417 (-0.7 %)	2.779 (-0.8 %)	2.859 (-2.5 %)	1.931 (-0.6 %)	1.790 (-0.2 %)	2.872 (0.0 %)
PBE	2.456 (0.9 %)	2.824 (0.8 %)	2.919 (-0.5 %)	1.959 (0.8 %)	1.815 (1.2 %)	2.919 (1.6 %)
PBE-D3	2.442 (0.3 %)	2.803 (0.1 %)	2.862 (-2.4 %)	1.946 (0.2 %)	1.808 (0.8 %)	2.909 (1.3 %)
HSE06	2.438 (0.2 %)	2.802 (0.0 %)	2.921 (-0.4 %)	1.944 (0.0 %)	1.797 (0.1 %)	2.912 (1.4 %)
HSE06-D3	2.420 (-0.5 %)	2.778 (-0.8 %)	2.851 (-2.8 %)	1.929 (-0.7 %)	1.788 (-0.4 %)	2.892 (0.7 %)
PBEsol	2.425 (-0.3 %)	2.796 (-0.2 %)	2.861 (-2.5 %)	1.940 (-0.1 %)	1.804 (0.5 %)	2.881 (0.3 %)

2.3 Changing geometry of TiO_5S octahedra in $\text{Y}_2\text{Ti}_2\text{S}_2\text{O}_5$ at different levels of lithiation

Table S3: Geometry of TiO_5S octahedra at different points along the convex hull from DFT results, compared with experiment.¹ The value in brackets is the % difference in the calculated interatomic distance, with respect to the comparative experimental distance.

x	Method	Ti-O _{a,b}	Ti-O1 (eq) (Å)	Ti-O2 (ax) (Å)	Ti-S (Å)
0	Expt. ¹		1.943	1.794	2.874
	DFT		1.944 (0.0 %)	1.797 (0.1 %)	2.912 (1.3 %)
0.99	Expt. ¹	<i>a</i>	1.957	1.886	2.679
1.00	DFT		1.935 (-1.1 %)	1.869 (-0.9 %)	2.619 (-2.2 %)
0.99	Expt. ¹	<i>b</i>	1.969		
1.00	DFT		1.953 (-0.8 %)		
1.52	Expt. ¹		1.970	1.932	2.587
1.50	DFT		1.966 (-0.2 %)	1.943 (0.6 %)	2.487 (-3.9 %)
1.85	Expt. ¹		1.980	1.950	2.512
2.00	DFT		1.976 (-0.2 %)	1.987 (1.9 %)	2.421 (-3.6 %)

2.4 Electronic density of states for $\text{Y}_2\text{Ti}_2\text{S}_2\text{O}_5$ and $\text{Li}_2\text{Y}_2\text{Ti}_2\text{S}_2\text{O}_5$ calculated using PBEsol.

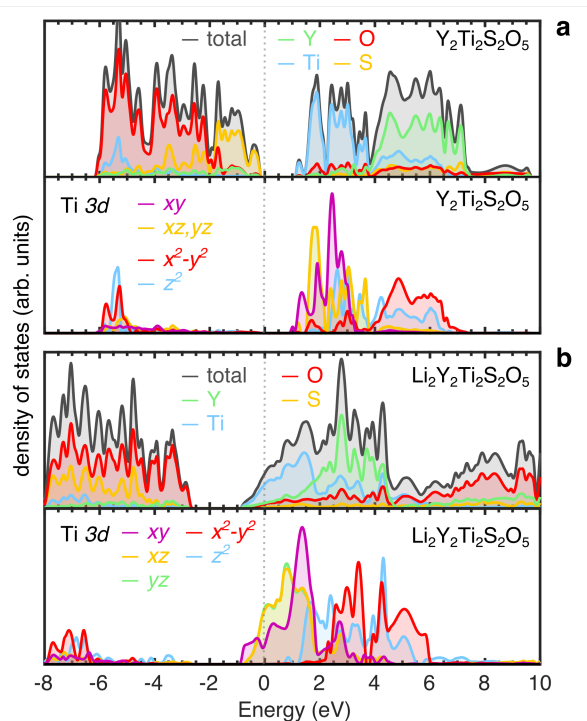


Figure S1: Electronic density of states for (a) $\text{Y}_2\text{Ti}_2\text{S}_2\text{O}_5$ and (b) $\text{Li}_2\text{Y}_2\text{Ti}_2\text{S}_2\text{O}_5$ calculated using PBEsol.

References

- [1] G. Hyett, O. J. Rutt, S. G. Denis, M. A. Hayward and S. J. Clarke, *J. Am. Chem. Soc.*, 2004, **2**, 1980–1991.